Geometrically biased random walks in bacteria-driven micro-shuttles

Geometrically biased random walks in bacteria-driven micro-shuttles

Luca Angelani[1] and Roberto Di Leonardo

CNR-IPCF, UOS Roma, c/o Dip. di Fisica, Università 'Sapienza',
I-00185 Roma, Italy
E-mail: luca.angelani@phys.uniroma1.it

Abstract. Micron-sized objects having asymmetric boundaries can rectify the chaotic motions of an active bacterial suspension and perform geometrically biased random walks. Using numerical simulations in a planar geometry, we show that arrow-shaped micro-shuttles, constrained to move in one dimension (1D) in a bath of self-propelled micro-organisms, spontaneously perform unidirectional translational motions with a strongly shape-dependent speed. Relaxing the 1D constraint, a random motion in the whole plane sets in at long times, due to random changes in shuttle orientation caused by bacterial collisions. The complex dynamics arising from the mechanical interactions between bacteria and the object boundaries can be described by a Gaussian stochastic force with a shape-dependent mean and a self-correlation decaying exponentially on the timescale of seconds.

S Online supplementary data available from stacks.iop.org/NJP/12/113017/mmedia

Contents

[1] Author to whom any correspondence should be addressed.

1. Introduction

Transporting objects in our macroscopic world is a common task that has been achieved with very high efficiency in different contexts and situations. Going down to the microscopic world, dominated by viscous forces over the inertial ones [1, 2], the problem has not yet been efficiently solved with artificial motors, while nature has found ingenious solutions such as the use of flagella or cilia in motile bacteria. Moving micro-cargoes or actuating micro-objects constitutes a very hard and intriguing challenge for present-day scientists, embracing many different disciplines, from basic physics to engineering and biology [3]. Potential applications, ranging from drug delivery to micro-fluidics and lab-on-chip technology, make the subject extremely appealing and of broad interest.

Strictly speaking, there are two main approaches for actuating micro-objects, basically differing in the nature of the power source used for the purpose. One approach makes use of externally controlled power sources, such as modulated electromagnetic fields: this is the case, for example, of magnetic snakes [4] or artificial bacterial flagella [5]. The other approach tries to build or assemble autonomous moving robots by integrating biological motors into nanofabricated structures [6, 7]. Until we are able to synthesize efficient artificial micro-motors, this latter strategy provides the most promising way to achieve self-propulsion of nanofabricated objects. In this respect, some preliminary reports on the actuation of micro-objects using motile bacteria have recently appeared in the literature. For example, it has been shown that polystyrene beads can be propelled by flagellated bacteria, resulting in a chaotic random motion [8, 9], or micro-rotary motors can be actuated by preferentially attaching cells onto the rotor edge [10]. Last year we proposed a new mechanism for such a task [11], in which a unidirectional rotational motion of a micro-gear emerges spontaneously by simply immersing the passive object into a bath of self-propelled micro-organisms, such as motile bacterial cells. Such a 'bacterial-ratchet effect', first obtained in numerical simulations, has been recently observed in experiments [12, 13], in remarkably good agreement with our original numerical prediction.

The proposed rectification process resembles very closely that described by Feynman in his famous 'Ratchet and pawl' lecture [14], where the second law of thermodynamics is discussed from a statistical mechanics point of view [15, 16]. The possibility of extracting work from a chaotic bath through a rectification process relies on both time-reversal and spatial-inversion symmetry breaking. The out-of-equilibrium properties of the bath (two thermal baths at different temperatures in the case described by Feynman and a bacterial bath with an intrinsically irreversible dynamics in our case) break the time-reversal symmetry and then the detailed balance, which in equilibrium ensures an equal probability for forward and backward trajectories. Once time inversion symmetry does not hold, a broken spatial inversion symmetry (an asymmetric shaped gear or shuttle) can lead to a rectification process [17].

In this paper, we investigate how such a 'bacterial-ratchet' mechanism can be used to propel micro-shuttles in a unidirectional translational motion. One key ingredient to obtain a directional motion is the asymmetric shape of the objects, whose boundaries provide concave-shaped sites that are able to trap bacteria in preferential propulsion positions. The particular asymmetry of the object determines the net direction of motion. The resulting swimming robot is propelled in a spontaneous way by the motile units, which constitute the 'fuel' for the micro-machine. Moreover, the motile units are in continuous chaotic motion, changing repeatedly their position and orientation, then allowing a sort of 'turnover' in their pushing task. This is an important and crucial point in real applications, as it allows us to neglect the effects of power off or low

efficiency of the single pushing unit. In this work, we perform simulations using planar geometry and considering different-shaped objects (rocket-like shuttles with back concave shape and with increasing number of teeth) immersed in a bacterial bath and constrained to move in one dimension. We analyze in detail the statistical properties of the applied forces and the resulting unidirectional object velocities in the various cases. When we relax the one-dimensional (1D) constraint and allow the shuttles to move in the whole plane, a linear motion is observed only at short times, whereas a random walk sets in at longer times, due to shuttle reorientation caused by the interactions with bacteria. Finally, we show that the 1D shuttle motion can be described by a Langevin-like equation driven by time-correlated random forces with a geometrically biased average.

2. Simulation

In our numerical simulation, elongated motile micro-organisms are modeled as self-propelled particles, which interact among themselves and with a single passive larger object [11]. The relevant Reynolds number, even when evaluated for the largest values of speed ($U \sim 30 \, \mu\text{m s}^{-1}$, bacteria speed) and length ($L \sim 40 \, \mu\text{m}$, largest object size), remains negligibly small ($Re = UL/\nu \sim 10^{-3}$). Each swimmer is described by two force centers at a fixed distance (bacteria with the aspect ratio 1/2) and an orientation unit vector $\hat{\mathbf{e}}$. The interaction (force and torque) between two swimmers is obtained from the resulting spherical interactions (soft potential repulsion $1/r^{12}$) among the different force centers. Each swimmer has a self-propulsion given by a constant force acting along the $\hat{\mathbf{e}}$ direction. The swimmer–object interaction is described by soft-potential repulsions between the force centers of the swimmer and the boundaries of the object. The equations of motion for the swimmers are

$$\begin{pmatrix} \mathbf{V}_i \\ \mathbf{\Omega}_i \end{pmatrix} = \begin{pmatrix} \mathbf{M}_i & 0 \\ 0 & \mathbf{K}_i \end{pmatrix} \cdot \begin{pmatrix} \mathbf{F}_i \\ \mathbf{T}_i \end{pmatrix}, \tag{1}$$

where the index i refers to the ith swimmer, $\mathbf{V}$ and $\mathbf{\Omega}$ are translational and angular velocities, $\mathbf{M}$ and $\mathbf{K}$ are translational and rotational mobilities and $\mathbf{F}$ and $\mathbf{T}$ are force and torque. Bacterial mobility matrices are given by $\mathbf{M}_i = m_{||}^{\text{b}} \hat{\mathbf{e}}_i \hat{\mathbf{e}}_i + m_{\perp}^{b} (\mathbb{1} - \hat{\mathbf{e}}_i \hat{\mathbf{e}}_i)$ and $\mathbf{K}_i = k_{||}^{\text{b}} \hat{\mathbf{e}}_i \hat{\mathbf{e}}_i + k_{\perp}^{b} (\mathbb{1} - \hat{\mathbf{e}}_i \hat{\mathbf{e}}_i)$, in which parallel and transverse bacterial scalar mobilities appear. We consider a planar geometry ($N = 1092$ bacteria in a box $L_{\text{b}} \times L_{\text{b}}$ at the concentration $\rho = N/L_{\text{b}}^2 = 1.05 \times 10^{-1} \, \mu\text{m}^{-2}$) and an external object constrained to move in one dimension (along the x-axis). An equivalent bulk concentration of bacteria could be estimated assuming a thickness for our simulation layer of about $3 \, \mu\text{m}$ (one bacterial length) that gives a bulk concentration of about 3.5×10^{10} bacteria ml^{-1}. The equation of motion of the micro-object is

$$v = m_{||} f, \tag{2}$$

where v is the x-velocity of the shuttle, $m_{||}$ its mobility along the x-axis and f the resulting force due to the pushing swimmers along its boundaries. Real swimming bacteria also undergo frequent tumbling events, during which flagellar motors reverse direction, flagella unbundle and the cell reorients randomly in space before starting a new linear run [18]. Tumbling events are reproduced in the simulation as short time intervals ($10^{-1} \, \text{s}$) where the propelling force is switched off and a random torque is applied to the cell body. The values of bacterial parameters are chosen to describe *Escherichia coli* cells: $\ell = 3 \, \mu\text{m}$ (bacterial length),
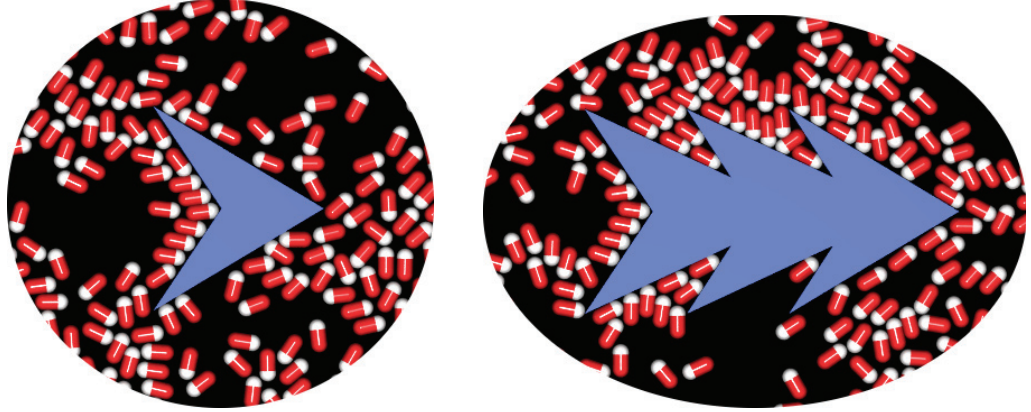
Figure 1. Snapshots taken from simulations of two different-shaped micro-shuttles immersed in bacterial baths. It is evident that there is a preferential alignment of bacteria along the symmetry axis of the shuttle, giving rise to a net pushing unidirectional force (towards the right in the present cases). See the supplementary movies available from stacks.iop.org/NJP/12/113017/mmedia.

Table 1. Values of the average force $\langle f \rangle$, velocity $\langle v \rangle$ and the corresponding variances σ_f and σ_v for the different bacterial-propelled shuttles with length L and mobility $m_{||}$.

Boats	L (μm)	$m_{||}$ (μm s^{-1} pN^{-1})	$\langle f \rangle$ (pN)	$\langle v \rangle$ (μm s^{-1})	σ_f (pN)	σ_v (μm s^{-1})
➤	15	5.90	0.52	3.1	0.71	4.0
➤➤	24	5.52	0.77	4.2	0.67	3.6
➤➤➤	33	5.04	1.0	5.2	0.55	2.9
➤➤➤➤	42	4.64	1.4	6.4	0.58	2.6

$v_0^b = 30\,\mu\text{m s}^{-1}$ (free bacterial velocity), $m_{||}^b = 58.8\,\mu\text{m s}^{-1}\,\text{pN}^{-1}$, $m_\perp^b = 51.3\,\mu\text{m s}^{-1}\,\text{pN}^{-1}$, $k_\perp^b = 31.3\,\mu\text{m s}^{-1}\,\text{pN}^{-1}$ ($k_{||}^b$ does not enter equation (1) in the planar geometry) and $\tau_{\text{tumble}} = 1$ s (mean tumbling time). Equations of motion (1) and (2) are numerically integrated using the Runge–Kutta method [19] (time step 10^{-4} s) for 40 s.

We consider different shuttles with back concave shape and a variable number of teeth (see, for example, figure 1 for the one- and three-tooth shuttles). Translational mobilities of the shuttles are estimated from analytical expressions for prolate spheroids with similar linear dimensions [2]. In table 1, length and mobility values are reported for the analyzed micro-objects.

3. Results

In figure 2, the probability distribution of forces exerted by bacteria on micro-shuttles is shown for the different analyzed cases. For each considered object, a set of 50 independent runs is considered (an example of the time-dependent fluctuating force measured in a single run is reported in the inset of figure 2 for the smallest shuttle case). The force distributions show a Gaussian shape centered at non-zero value (means $\langle f \rangle$ and variances $\sigma_f = \langle f^2 \rangle - \langle f \rangle^2$ are
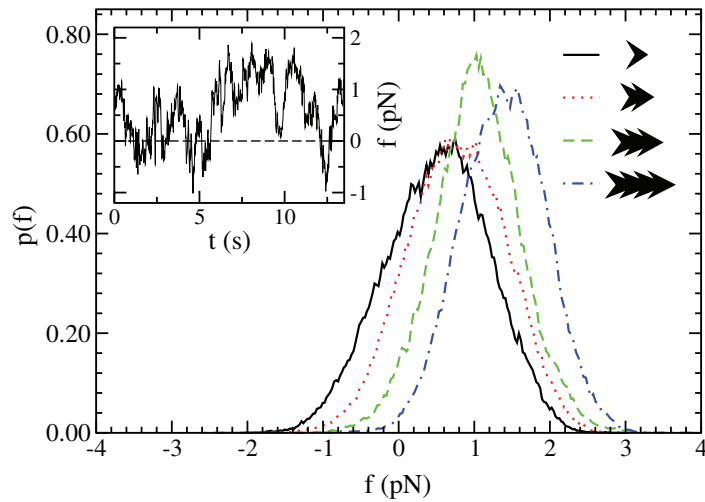
Figure 2. Probability distribution of the forces exerted by bacteria on different micro-shuttles. Inset: an example of the time variation of the force f in a single run for the smallest shuttle case.

reported in table 1), indicating a net unidirectional average force on the objects. This is due to the preferential trapping and alignment of self-propelled units in the back side of the shuttles, while bacteria tend to flow away from the other boundaries, giving rise to a non-vanishing net propelling force. The above trapping mechanism can be understood by considering the interactions between cells and the object boundaries. They are described by repulsive contact forces directed along the surface normal: when a micro-organism hits a boundary, it aligns and slides parallel to it until it gets stuck in a corner in a 'pushing' configuration (see figure 1). Interactions with other cells or tumbling events can eventually set free the pushing cell to swim back into the solution. Only concave corners support such an alignment and pushing mechanism, as observed also in previous investigations (see, for example, figure 3 in [11] or figure 2 in [12]). In the case of many teeth (right panel in figure 1), such an alignment process takes place for every concave-shaped boundary between adjacent teeth. One then expects a growing net force with the number of teeth. This is indeed the case, as is shown in figure 3, where the average force is reported as a function of teeth number (full symbols in the figure). The data show a linear trend with the slope $\Delta f = 0.29$ pN, which represents the contribution of a single tooth to the net force, while the value $f(1) = 0.49$ pN is the average contribution of the concave back side. The resulting averaged shuttle velocities are reported as open symbols in figure 3, and the numerical values $\langle v \rangle$ and σ_v are shown in table 1. It is worth noting that, in contrast to the average forces and velocities, the variances of probability distributions (see figure 2 and table 1) do not show a clear monotonic trend with increasing number of teeth.

The possible dependence of the reported values on bacterial bath properties has been checked by considering a different bacterial density and the suppression of tumbling. Changing the bacterial concentration (density $\rho = 0.077\,\mu\mathrm{m}^{-2}$), one obtains $\langle f \rangle \simeq 0.52$ pN and $\langle v \rangle \simeq 3.0\,\mu\mathrm{m\,s}^{-1}$. Then, the bacterial density seems to not affect shuttle motion (at least at the considered concentration variability) in agreement with the fact that bacteria tend to accumulate close to surfaces [20, 21] and, irrespective of the overall number density, they form aggregates with the same local concentration around the object. When suppressing the
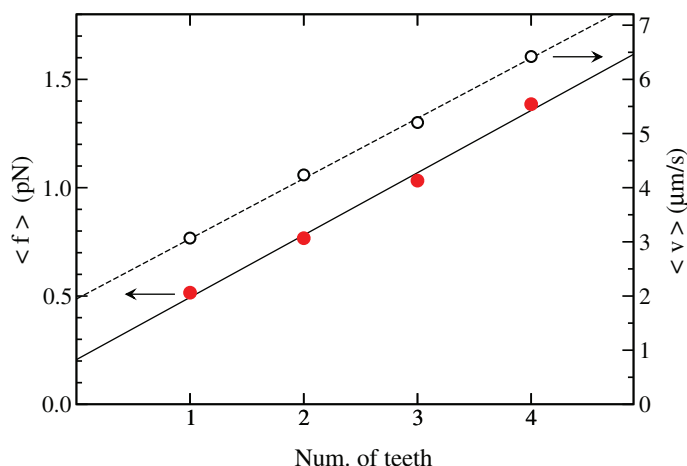
Figure 3. The average force $\langle f \rangle$ exerted on micro-shuttles by motile bacteria (full symbols, left axis) and the resulting average shuttle velocity $\langle v \rangle$ (open symbols, right axis) as a function of the number of shuttle teeth. The slope of the continuous line is $\Delta f = 0.29$ pN, representing the force contribution of a single tooth, while the value $f(1) = 0.49$ pN represents the force contribution of the concave back side.

tumbling mechanism, one observes $\langle f \rangle \simeq 1.4$ pN and $\langle v \rangle \simeq 8.3\,\mu\mathrm{m\,s}^{-1}$. Tumbling has then a relevant effect on shuttle velocity: when immersed in a bath with bacteria without tumbling, the shuttle moves about three times as fast as in the previous case. A simple explanation for this can be obtained by considering the pushing bacteria stuck in the concave parts of the shuttle boundaries. Their pushing task is interrupted by a reorientation of their swimming direction, which causes the cell to swim back into the solution and leave empty the pushing position until another cell occupies it. The efficiency of the pushing task is then controlled by the timescale of cell reorientation. The latter can be due to two main mechanisms: the interaction with other cells or the tumbling event. Considering cells without tumbling removes a possible cause of efficiency loss, giving rise to more persistent pushing bacteria and then faster shuttles.

Time-dependent correlation functions give insight into the dynamics of the shuttles. We have analyzed the force–force correlation function $C_f(t) = \langle f(t_0) f(t_0 + t) \rangle - \langle f \rangle^2$, which, in the stationary regime, does not depend on t_0. In figure 4, the normalized function $C_f^N(t) = C_f(t)/C(0)$ is shown for the different shuttles (averaged over initial time t_0 and over 50 independent simulation runs). All the data seem to superimpose and can be fitted with a unique curve, confirming that dynamics of force fluctuations can be regarded as a property of the bath alone, as already observed in [12]. A simple exponential fit $g(t) = \exp[-t/\tau]$ (with $\tau = 1.27$, dashed line in the figure) reproduces quite well the long-time behavior. However, a stretched-exponential fit-function $g(t) = \exp[-(t/\tau)^\beta]$ (with $\tau = 1.36$ s and $\beta = 0.825$, continuous line in the figure) seems to reproduce more accurately the overall range. We have to mention that also a fit with two exponential functions (not shown in the figure) agrees equally well. The exact analytical form of the correlation is then quite difficult to establish with high precision from the data; however, we can conclude that the long-time decay is nearly exponential with a relaxation time of about 1.3 s. It is worth noting that τ is very close to the mean tumbling time $\tau_{\mathrm{tumble}} = 1$ s, indicating such a mechanism as the main reason for the force decorrelation. In the inset of figure 4, a comparison between the tumbling and no-tumbling cases is reported
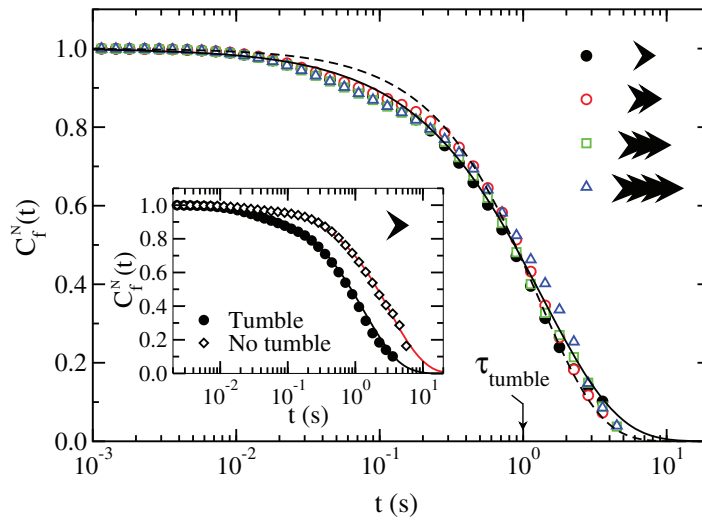
Figure 4. The normalized force correlation function $C_f^N(t) = C_f(t)/C(0)$, with $C_f(t) = \langle f(t_0) f(t_0 + t) \rangle - \langle f \rangle^2$ for the different shuttles. Lines are fits to an exponential function $g(t) = \exp[-t/\tau]$ ($\tau = 1.27$, dashed line) and a stretched-exponential function $g(t) = \exp[-(t/\tau)^\beta]$ ($\tau = 1.36\,$s and $\beta = 0.825$, continuous line). Inset: the same for the smallest shuttle with and without tumble (for the latter the stretched-exponential fit gives $\tau = 3.26\,$s and $\beta = 0.860$).

for the smallest shuttle. The latter shows a longer decorrelation time ($\tau = 3.26\,$s), which can be attributed to the interactions among bacteria, lacking in this case tumbling-decorrelation events.

We now relax the 1D constraint and allow the shuttle to move in the whole 2D plane. In the main panel of figure 5, the probability distributions of forces (parallel $f_{\parallel}$ and transverse $f_{\perp}$ with respect to the object symmetric axis) are shown for the case of the smallest shuttle. It is evident that there is a non-zero mean value of the parallel force, while there is a zero mean value of the transverse one, indicating, also in this unconstrained case, a geometrically biased random force acting on the object. The asymmetric shape is a crucial point, as is evident from an analysis of a symmetric shuttle, figure 5(b), for which both parallel and transverse force distributions are symmetric. However, whether symmetric or not, the objects now move in a plane, so rotations are also important. Indeed, the torque exerted by colliding bacteria causes rotations of the shuttle, destroying any possible unidirectional motion—see figure 5(c) for the torque distributions for asymmetric and symmetric shuttles. In figure 6, the orientational correlation function $C_e(t) = \langle \hat{\mathbf{e}}(t_0) \cdot \hat{\mathbf{e}}(t_0 + t) \rangle$ of the free shuttle ($\hat{\mathbf{e}}$ is the orientation unit vector) is shown as a function of time. It decays to zero at about 10 s, indicating that above such a time the shuttle loses memory of its initial orientation. As an example, in the inset of figure 6 two trajectories in the (x, y)-plane performed by free shuttles are depicted.

4. Effective Langevin equation

The above-reported findings suggest that it is possible to describe the shuttle motion in the 1D case in terms of an effective Langevin equation (in the overdamped regime)

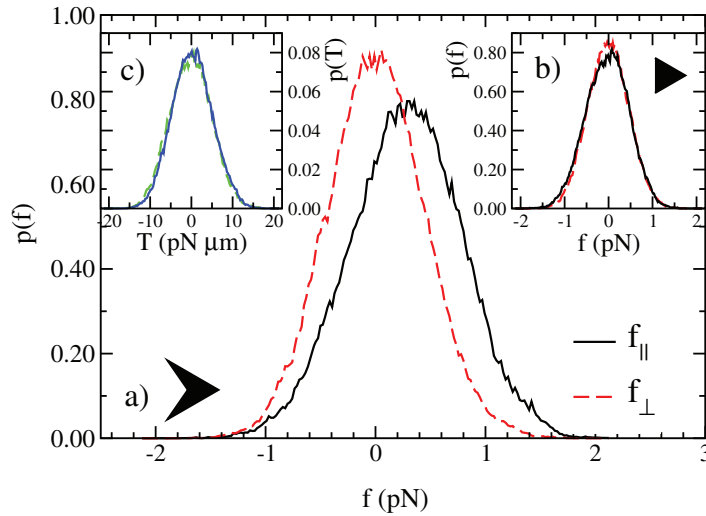$$\frac{\mathrm{d}x}{\mathrm{d}t} = m_{\parallel} f, \tag{3}$$

Figure 5. Free shuttles moving in a 2D plane. (a) Probability distribution of parallel $f_{\parallel}$ (continuous black line) and transverse $f_{\perp}$ (dashed red line) forces (with respect to the object's symmetry axis) for the asymmetric shuttle. (b) The same for a symmetric triangular shuttle. (c) Probability distribution of torques for asymmetric (continuous blue line) and symmetric (dashed green line) shuttles.
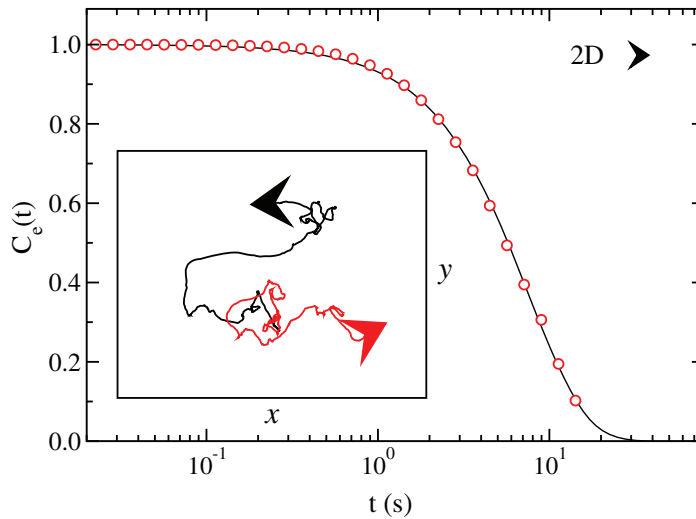

Figure 6. The orientational correlation function $C_e(t) = \langle \hat{\mathbf{e}}(t_0) \cdot \hat{\mathbf{e}}(t_0 + t) \rangle$ for a free shuttle moving in the whole 2D plane ($\hat{\mathbf{e}}$ is the orientation unit vector of the shuttle) is shown in the main figure. The line represents a stretched-exponential fit $g(t) = \exp[-(t/\tau)^{\beta}]$ ($\tau = 7.6$ s and $\beta = 1.3$). Inset: an example of two shuttle trajectories in the (x, y) plane lasting 40 s.

where f is a random force with non-zero mean (effect of unidirectional pushing bacteria) and is time correlated (due to bacterial interactions and/or tumbling events):

$$\begin{cases} \langle f(t) \rangle = f_0, \\ \langle f(t) f(t') \rangle = f_0^2 + \sigma_f^2 \, g(t - t'). \end{cases} \tag{4}$$
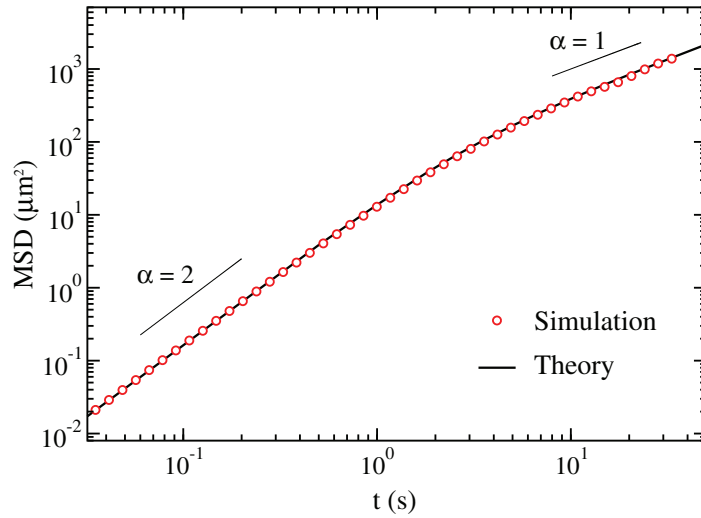
Figure 7. Mean square displacement $\Delta x^2 - \langle v \rangle^2 t^2$ for the smallest shuttle. Symbols are from simulation and the line is the theoretical expression in equation (6), without the first quadratic term in the rhs (parameters are taken from table 1 and figure 4).

The function g is assumed to be exponential $g(t - t') = e^{-|t-t'|/\tau}$, in quite good agreement with numerical findings. Parameter values (f_0, σ_f, τ) depend on shuttle shape as well as bacterial bath properties. In such approximations, the average shuttle position $\Delta x(t) = \langle x(t_0 + t) - x(t_0) \rangle$ and the mean square displacement $\Delta x^2(t) = \langle |x(t_0 + t) - x(t_0)|^2 \rangle$ are given by

$$\Delta x(t) = \langle v \rangle t = m_\parallel f_0 t, \tag{5}$$

$$\Delta x^2(t) = m_\parallel^2 f_0^2 t^2 + 2m_\parallel^2 \sigma_f^2 \tau [t - \tau(1 - e^{-t/\tau})] \tag{6}$$

In figure 7, the measured mean square displacement for the smallest shuttle is reported together with the analytical expression (6), using the parameter values obtained previously. Both are obtained considering only the non-trivial diffusive term, i.e. $\Delta x^2 - \langle v \rangle^2 t^2$. A transition from the ballistic (t^α, with $\alpha = 2$) to the diffusive ($\alpha = 1$) regime is observed at about 2 s. The good agreement between simulation data and the theoretical expression suggests that the effective Langevin equation with exponentially correlated random forces well describes the shuttle motion in the whole range. The resulting diffusion coefficient $D = \lim_{t \to \infty} [\Delta x^2 - (\Delta x)^2]/(2t)$ estimated from the data is $D \simeq 22.3 \, \mu\text{m}^2 \, \text{s}^{-1}$, about three orders of magnitude greater than the thermal one $D_\text{T} = k_\text{B}T/(6\pi\mu_w R) \simeq 0.029 \, \mu\text{m}^2 \, \text{s}^{-1}$ (obtained for a spherical particle of radius $R = L/2$ in water at room temperature). This is consistent with previous findings on enhanced purely diffusion transport of symmetric beads in active suspensions [9, 22].

The general 2D case (shuttle motion allowed in the whole plane) is expected to be described by a similar Langevin equation, now with two random forces (a parallel one, with respect to the object symmetry axis, having non zero mean and a perpendicular one with zero mean) plus a random torque (with zero mean) responsible for the decorrelation of the object orientation and then for the break in directional motion in this case.

5. Conclusions

By using numerical simulations, we have analyzed the motion of different-shaped objects immersed in a bath of self-propelled units, mimicking living motile micro-organisms such as *E. coli*. The object shape induces preferentially directional motion, due to concave-shaped boundaries where motile bacteria are trapped for a long time and cooperatively push the object. In the analyzed 1D case, this mechanism allows unidirectional motion of the considered object, obtained by simple immersion in the active bath. The 1D case can be experimentally obtained by geometric/mechanical constraints (motion of objects along a small channel) or by aligning magnetic objects with external magnetic fields. The finding is robust against variation of bacterial bath parameters, such as the concentration or tumbling mechanism, with only possible quantitative differences. Relaxing the 1D constraint, one observes again a net preferential motion along the symmetric axis of the shuttles; however, the latter changes direction in a random way due to the stochastic interactions with the bacteria in the transverse direction: as a result, the object's motion is no longer unidirectional, but resembles that of a self-motile colloidal particle [23]. Detailed analysis of statistical properties (distributions of forces and velocities, time correlation functions) allows us to describe the object motion in the 1D case in terms of an effective Langevin-like equation, with a random force having non-zero mean and correlated in time. The above mechanism can provide a novel strategy to propel micro-objects or cargoes at the micrometer scale, with possible applications in hybrid micro-device engineering, lab-on-chip technology, micro-fluidics and drug delivery.

Acknowledgments

References

[1] Purcell E M 1976 *Am. J. Phys.* **45** 3
[2] Kim S and Karrila S J 2005 *Microhydrodynamics* (New York: Dover)
[3] Ebbens S J and Howse J R 2010 *Soft Matter* **6** 726
[4] Snezhko A, Belkin M, Aranson I S and Kwok W K 2009 *Phys. Rev. Lett.* **102** 118103
[5] Zhang L, Abbott J J, Dong L, Kratochvil B E, Bell D and Nelson B J 2009 *Appl. Phys. Lett.* **94** 064107
[6] Steager E, Kim C B, Patel J, Bith S and Naik C 2007 *Appl. Phys. Lett.* **90** 263901
[7] Darnton N, Turner L, Breuer K and Berg H C 2004 *Biophys. J.* **86** 1863
[8] Weibel D B, Garstecki P, Ryan D, DiLuzio W R, Mayer M, Seto J E and Whitesides G M 2005 *Proc. Natl Acad. Sci. USA* **102** 11963
[9] Behkam B and Sitti M 2007 *Appl. Phys. Lett.* **90** 023902
[10] Hiratsuka Y, Miyata M, Tada T and Uyeda Q P 2006 *Proc. Natl Acad. Sci. USA* **103** 13618
[11] Angelani L, Di Leonardo R and Ruocco G 2009 *Phys. Rev. Lett.* **102** 048104
[12] Di Leonardo R *et al* 2010 *Proc. Natl Acad. Sci. USA* **107** 9541
[13] Sokolov A, Apodaca M M, Grzybowski B A and Aranson I S 2010 *Proc. Natl Acad. Sci. USA* **107** 969
[14] Feynman R P, Leighton R B and Sands M 1966 *The Feynman Lectures on Physics* vol I (Reading, MA: Addison-Wesley) chapter 46

[15] Reimann P 2002 *Phys. Rep.* **361** 57
[16] Berger J 2004 *Entropy* **6** 68
[17] Curie P 1894 *J. Physique* III **3** 393
[18] Berg H C 2004 *E. Coli in Motion* (New York: Springer)
[19] Press W H, Vetterling W T, Teukolsky S A and Flannery B P 1992 *Numerical Recipes in C* (New York: Cambridge University Press)
[20] Berke A P, Turner L, Berg H C and Lauga E 2008 *Phys. Rev. Lett.* **101** 038102
[21] Li G and Tang J X 2009 *Phys. Rev. Lett.* **103** 078101
[22] Darnton N, Turner L, Breuer K and Berg H C 2004 *Biophys. J.* **86** 1863
[23] Howse J R *et al* 2007 *Phys. Rev. Lett.* **99** 048102